Iranian Journal of Catalysis 6(3), 2016, 305-311

IRANIAN JOURNAL OF CATALYSIS

Effects of Ag, Nd codoping on structural, optical and photocatalytic properties of TiO_2 nanocomposite synthesized via sol-gel method using starch as a green additive

Bahar Khodadadi*

Department of Chemistry, Faculty of Science, University of Qom, Qom, Iran.

Received 24 April 2016; received in revised form 6 June 2016; accepted 22 June 2016

ABSTRACT

In this paper, undoped TiO_2 and Ag-Nd-codoped TiO_2 nanocomposites with different molar ratios of dopants were synthesized by the sol-gel method using starch as a natural additive. Structures were investigated by FT-IR and UV–Vis spectroscopy, SEM, and XRD methods. Moreover, the direct band gap was calculated by Tauc's approach. Furthermore, photocatalytic activity of all samples were investigated under UV irradiation in an aqueous medium. Compared with undoped TiO_2, the band gap of the Ag-Nd -TiO_2 samples decreases and depends on the content of dopants. In addition, photocatalytic activity improves in the presence of appropriate amount (1.5 mol%) of Ag and Nd as dopants.

***Keywords**: Ag -Nd- TiO_2 nanocomposite, Band gap, Phptocatalytic activity, Sol-gel method.*

1. Introduction

Titanium oxide (TiO_2) has been considered a promising photocatalyst owing to its potential application in removing of all types of organic pollutants. Various organic dyes are widely used by many industries such as plastic, cosmetic, leather, textile, food and pharmaceutical in the form of colored wastewater. It is estimated that 15 % of these dyes are released to wastewater during dyeing process [1]. Therefore, water pollution due to the release of toxic chemicals from industrial sectors has been of major concern in recent years [2]. The preferential photocatalytic activity and popularity of nano sized TiO_2 for degradation of organic dyes is based on its large surface area to volume ratio, high oxidative power, photochemical stability, non-toxicity and low cost [3-7]. However, TiO_2 band gap is so large (Eg = 3.20 eV) to be only excited under UV light with a wavelength less than 387.5 nm. In addition, low quantum efficiency due to high recombination of photo generated electron-hole pair greatly limits its practical applications [8,9]. In order to improve the photocatalytic activity of TiO_2 and enhance the separation of electron hole pairs, numerous methods can be used including increase of surface area using additives, transition metals and rare-earth metal doped TiO_2. Among transition metals, Ag is expected to be a good candidate. It seems that Ag doping on TiO_2 leads to various effects on photocatalytic activity including enhancement of the electron-hole separation by acting as an electron trap and increasing surface electron excitation. Moreover, the use of Nd as a dopant causes a localized charge perturbation during substitutional doping into TiO_2 lattice to increase its photocatalytic activity [7-11].

To date, sol-gel technique has been one of the best methods generally employed for the preparation of TiO_2. This technique is very suitable due to its many advantages such as good homogeneity, low temperature synthetic conditions, low equipment cost and easily controlled reaction parameters [12,13].

Up to now, there have been many reports on the photocatalytic activity or antibacterial behavior of Ag or/and Nd doped TiO_2 nanoparticles [1-3,6,7,9,12, 14,16,17]. However, there have been no reports on the photocatalytic activity and the synthesis of an Ag, Nd-codoped TiO_2 nanocomposite via sol-gel technique

*Corresponding author email: khodadadi@qom.ac.ir
Tel.: +98 25 3210 3792; Fax: +98 25 3285 0953

using starch, an important natural organic compound abundant in nature, as a modifier used for controlling morphology of nanostructure [14]. Hence, in this study, we report a facile sol-gel method to synthesize Ag, Nd-codoped TiO_2 nanocopmosites (with different molar ratios). Moreover, starch is used as a natural organic polymer for preventing agglomeration of samples and modifying photocatalytic activity. The absorption spectra of the samples were measured and the variations in the optical band gap were analyzed. Morphology and sample structures were investigated by IR spectroscopy, Scanning Electron Microscopy (SEM), and X-Ray Diffraction (XRD) methods.

The photocatalytic activity of the Ag, Nd-codoped TiO_2 nanocomposites was found to be further enhanced owing to the narrowing band gap by doping appropriate amounts of Ag and Nd. In addition, Ag and Nd doping can suppress the electron/hole recombination through facilitating charge rectification and codoping can increase the TiO_2 surface area by hindering the growth of large TiO_2 particles [15].

2. Experimental

2.1. Materials and equipment

Titanium tetraisopropoxide (TTIP) (AR analytical grade, Merck Chemical Company) was the titanium source. Neodymium (III) nitrate hexahydrate ($Nd(NO_3)_3.6H_2O$), Silver nitrate ($AgNO_3$), glacial acetic acid, diethanolamine (DEA), absolute ethanol, and methyl orange were purchased from Merck Chemical Company. Deionized water, starch and acetone (for drying) were used without any further purification. The sample structures were characterized by X ray diffraction pattern recorded on a Philips model X'Pert Pro diffractometer employing Cu Kα radiation (λ=1.5418Å), while the morphologies of the synthesized samples were investigated by field emission scanning electron microscopy (SEM; KYKY-EM 3200) equipped with an Oxford Inca Energy Dispersive X-ray detector. UV-Vis spectra were recorded by using a Shimadzu UV-2500 spectrophotometer in the wavelength range of 200-700 nm. Fourier transform infrared spectroscopy (FT-IR) analysis was carried out on a FT-IR (Jasco, 4200) spectrophotometer to determine the specific functional groups present on the surface and impurities of synthesized samples.

2.2. Sample preparation

In a typical synthesis, samples were synthesized by the following procedure:

First, 0.2 g of starch was dissolved in 30 mL of absolute ethanol and stirred for 10 min using a homogenizer. 10 mL of TTIP was then added to the solution and stirring continued for 15 min (solution I). Next, equal amounts of $Nd(NO_3)_2.6H_2O$ and $AgNO_3$. H_2O as dopant were dissolved in 5 mL of absolute ethanol (with molar ratio of Ag/Ti and Nd/Ti = 0.075, 0.015 and 0.03, respectively), followed by addition of 0.2 mL of double distilled water and 0.8 mL of diethanolamine (DEA) to the solution. It was stirred for 5 min (Solution II). Finally, solution II was added dropwise into Solution I and the resulting solution was vigorously stirred for 15 min.

The obtained transparent colloidal suspension was then sonicated for 30 min and aged to allow a gel to form. The sample was dried in an oven at 50ºC and ultimately calcinated at 500ºC for 3 hours.

2.3. Photocatalytic conditions

Methyl orange (MO) has often been used as a model dye for photocatalytic degradation examination of samples. The photocatalytic activity of pure TiO_2 and Ag, Nd-codoped TiO_2 samples was evaluated by examining photocatalytic decomposition of MO dye under UV irradiation. These nanostructures could be utilized in numerous applications, especially for photodegradation of organic pollutants [14]. All experiments were carried out in a photoreactor system with a capacity of 1 liter. MO (with a concentration of 5 mg L^{-1}) in deionized water was selected as the pollutant solution for photodegradation. These solutions were set left in the vicinity of a nano photocatalyst powder (0.2 g powder in 1 L solution) and were left in the dark for 24 h to eliminate the absorptive effect of the solution in the catalyst. The solutions were then placed in the photoreactor and MO concentration change was recorded by UV spectroscopy. The photoreactor system consisted of a cubic borosilicate glass reactor with an effective volume of 1000 mL, a cooling water jacket and a 15 W UV lamp (Osram) with a quartz cover positioned inside the solution used as a UV light source. The reaction temperature was kept at 25°C using cooling water. The progress of the conversion reaction was then monitored by UV–Vis absorption spectroscopy of the mixture using a spectrophotometer.

3. Results and Discussion

3.1. Sample characterization

Fourier transform infrared (FTIR) spectroscopy was carried out for characterization of functional groups at room temperature in the range of 400–4000 cm^{-1}. Results are shown in Fig. 1.

According to the results, the FTIR spectra of undoped, and Nd, Ag codoped TiO_2 are similar in nature to those of the undoped TiO_2 sample. In the region below 1000 cm^{-1}, all the spectra show main bands in the region between 400–700 cm^{-1}, which can be attributed to the Ti–O stretching and Ti–O–Ti bridging modes [16-20]. Moreover, the broad absorption peak at 1620 cm^{-1} corresponds to H–O–H bending vibration of physically

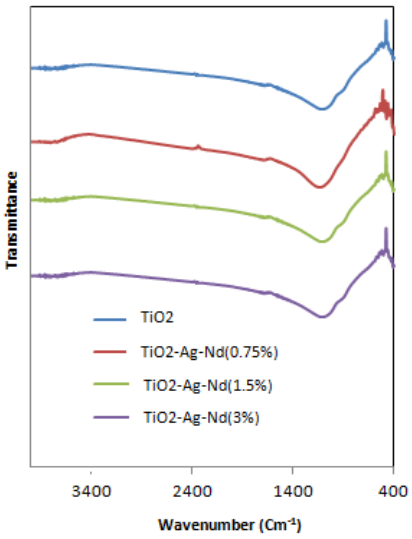

Fig. 1. FT-IR spectra of undoped and Ag-Nd-TiO_2 samples.

adsorbed water. In addition, the strong absorption band between 400 and 600 cm^{-1} corresponds to the stretching and vibrational modes of metal–oxygen (Ti-O, Ag–O or Nd-O) [2, 20-25].

X-ray diffraction analysis was employed to determine the crystal phase of the samples. The XRD patterns of the undoped and Ag-Nd codoped TiO_2 samples are shown in Fig. 2 [15].

The diffraction patterns of TiO_2 sample match with JCPDS card of TiO_2 (No. 04-0477) quite well. This pattern can be indexed to those of Tetragonal anatase structure [2,14,26,27]. The comparison of the spectrum of undoped TiO_2 and Ag-Nd codoped samples with different molar ratios of dopant also shows similar patterns, which indicates that the samples are single-phase with a Tetragonal anatase. However, no intense diffraction peaks related to the oxides of Ag and Nd have been observed. This is possibility due to the low amount of the dopant. XRD is unable to detect the diffraction peaks of the impurity [27,28].

According to XRD results, in comparison to the undoped sample, diffraction peak intensities of the codoped TiO_2 are reduced. It seems that the reduction in intensity on codoping is due to the inhibition of crystal growth and the increase of structural defects, particularly oxygen defects on the grain boundary and the lattice of TiO_2 [2,27]. Furthermore, careful observation of XRD pattern revealed that diffraction peaks of the Ag-Nd-codoped TiO_2 samples were shifted to lower diffraction angles with the increasing dopant molar ratio.

It is worth noting that the ionic sizes of Ag^+ (1.15A˚) and Nd^{3+} (0.983A˚) are larger than that of Ti^{4+} (0.605A˚). There is less possibility of all the added dopants to substitute Ti^{4+} in TiO_2. However, it seems that a few larger dopant ions can be substituted on Ti^{4+} site, causing the diffraction peak to shift to a lower angle. Moreover, it is reasonable to assume that most of the dopant ions are doped on the surface of TiO_2 lattice [2].

The lattice parameters of TiO_2 and Ag-Nd-TiO_2 samples with different dopant molar ratios were calculated from the XRD using the following equation [29].

$$\frac{1}{d^2} = \frac{4}{3}\left(\frac{h^2+kh+k^2}{a^2}\right) + \frac{l^2}{c^2}$$

where h, k and l are Miller indexes and d is distance between adjacent lattice planes in the crystal. Table 1 shows the calculated lattice parameters of the samples. Lattice parameters of codoped samples were slightly more than those of undoped TiO_2, confirming that a few of dopant ions have been doped into the TiO_2 crystal lattice without changing the anatase structure [30].

Fig. 3 illustrates FE-SEM images of the undoped and codoped samples. Results show that aggregated particles with a larger size are formed for undoped TiO_2 sample and can be easily observed by SEM image.

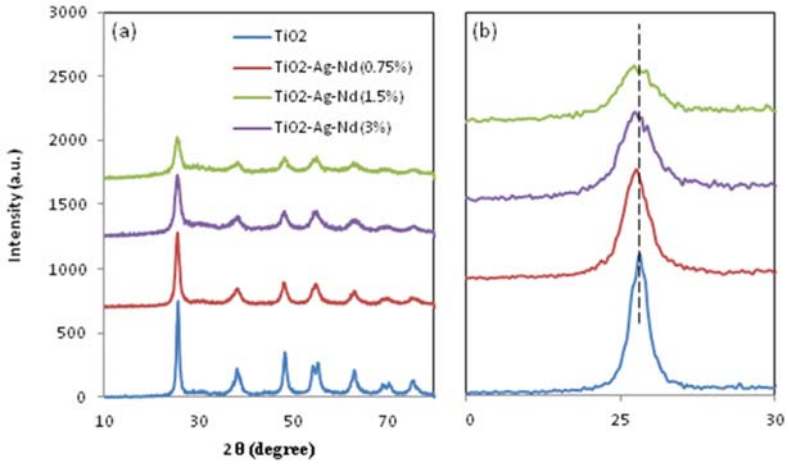

Fig. 2. XRD spectrum and peak position shifting of undoped and Ag-Nd-TiO_2 samples.

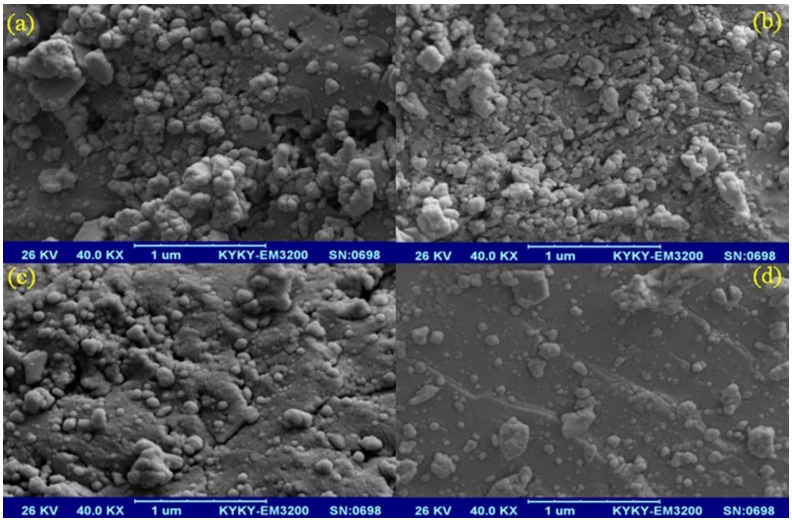

Fig. 3. SEM images of samples: (a) undoped TiO_2, (b) TiO_2- Ag-Nd (0.75 %), (c) TiO_2- Ag-Nd (1.5 %) and (d) TiO_2- Ag-Nd (3 %).

Moreover, it was found that the surface morphology and the particle size of the aggregated TiO_2 samples show no obvious change following modification by Ag and Nd to form codoped samples. However, it seems that co-doping can restrain the decrease in the diameter of particles and obtained nanoparticles are of more uniform shapes and sizes [26,31].

3.2. Optical properties of samples

UV–Vis absorption spectroscopy was performed to investigate the optical properties of synthesized samples. Fig. 4 shows the UV-Vis spectra of the different samples.

As observed in Fig. 4 (a), all synthetic samples exhibit a single and well-defined absorption band at around 340 nm, which is associated with the anatase structure of TiO_2. Moreover, compared to undoped TiO_2, the absorption edge shifts towards longer wavelengths for Ag-Nd-TiO_2 sample. [8].

The wavelengths of maximum absorbance for each sample are listed in Table 1 [27]. This shift in absorption edge for samples may be due to the introduction of the impurity levels with Ag and Nd doping. Moreover, from the absorption spectra, it can be concluded that Ag and Nd ions are well incorporated into the crystalline environment of TiO_2 and form band states of Ag and Nd in the band gap of the TiO_2 [8,27]. The weak peaks in the absorbance spectra in the visible region are attributed to f–f electronic transition of Nd^{3+} in the coordination environment of TiO_2 nanostructures [27,28].

Tauc's approach was used to investigate the absorption coefficients of samples, and the following equation was used in the calculation of the optical band gap of the undoped and Ag-Nd codoped TiO_2 with various molar ratios of dopant:

$$(\alpha h\nu)^2 = C\,(h\nu - E_g)$$

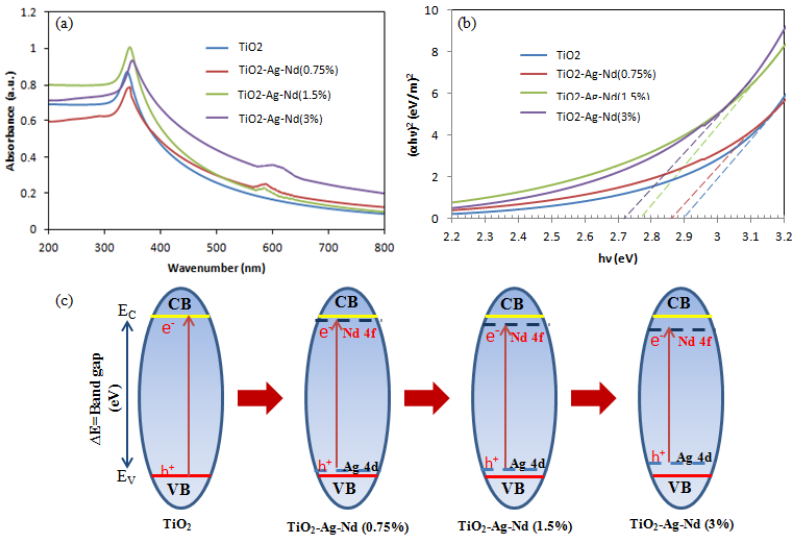

Fig. 4. (a) UV-Vis absorption spectrum, **(b)** the Tauc plots and **(c)** energy diagram of samples.

Table 1. Peak position, band gap, mean crystal size and lattice constants of samples.

Samples	(101) Peak position (degree)	a (100) (Å)	c (002) (Å)	Mean crystal size (nm)	Wavelength (nm)	Bandgap (eV)
TiO_2	25.652	3.3760	9.4860	40.20	339	2.90
TiO_2- Ag-Nd (0.75%)	25.354	3.3830	9.5100	38.70	342	2.86
TiO_2- Ag-Nd (1.5%)	25.325	3.7832	9.5123	36.50	344	2.78
TiO_2- Ag-Nd (3.0%)	25.279	3.7856	9.5139	34.30	347	2.72

where α is the absorption coefficient, C is a constant, hν is the photon energy and E_g is the band gap. Fig. 4 shows the Tauc plots of the samples. A band gap is obtained by extrapolation of the linear region of Tauc plot [12,32,48].

The energy band gap values for the undoped TiO_2 and Ag-Nd codoped TiO_2 nanoparticles were found to be approximately 2.90, 2.86, 2.78 and 2.72 eV, respectively. It was observed that the doping of TiO_2 with transition metals (Ag and Nd) resulted in a decrease in the band energy [33].

It is evidenced that upon increase of the Ag and Nd codoping content, the absorption edge shifts towards a longer wavelength, which indicates the decrease of the band gap [34]. These results indicate that the electrons of codoped samples can be excited with a lower energy from the valence band (VB) to these levels rather than the conduction band (CB) of the semiconductor due to formation of 4f Nd and 4d Ag states very near and below the CB edge. This shows that electron transition takes place from O 2p to Nd 4f level or Ag 4d can occur more easily. The energy diagram of the samples is shown in Fig. 4 [35-41].

3.3. Photocatalytic activity

The photocatalytic properties of undoped and Ag-Nd codoped TiO_2 nanocomposites were examined based on methyl orange (MO), which was used as a model dye for photocatalytic degradation of samples under UV irradiation.

Fig. 5 shows the change in concentration of MO for different time intervals. The results show that appropriate amounts of Ag and Nd as dopants have a beneficial effect on MO decomposition. According to the results, the sample containing 1.5 mol % of dopants had the highest photocatalytic activity. Slightly worse results were obtained for the TiO_2 (0.75 mol % Ag, Nd), undoped TiO_2 and, TiO_2 (3.0 mol % Ag, Nd) respectively.

Fig. 6 exhibits the proposed mechanism for improved photocatalytic activity of codoped TiO_2 samples. Several factors such as crystallinity, surface area, the electron-hole pair production capacity, and recombination of photogenerated electrons and holes are well known to play important roles on the photocatalytic property of TiO_2. Moreover, lattice defects such as oxygen vacancy could serve as favorable trap sites of the electrons or holes to reduce their recombination and, consequently, increase the photocatalytic activities.

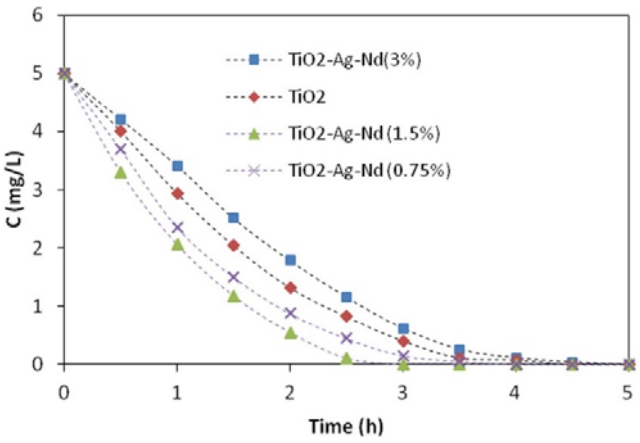

Fig. 5. Photodegradation of methyl orange (MO) using the samples.

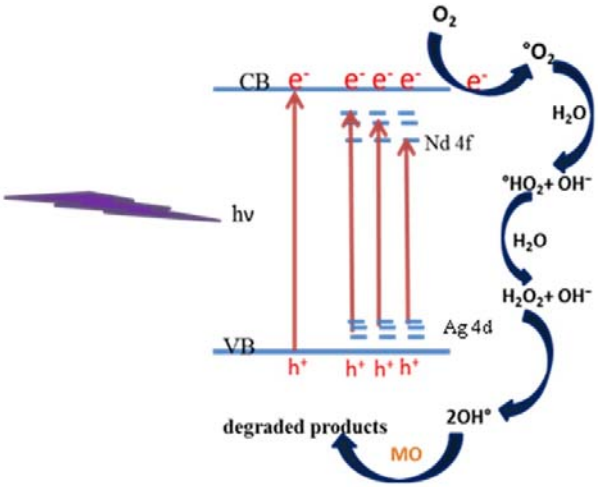

Fig. 6. Schematic illustration of the mechanism for photocatalytic activity of codoped TiO_2 samples.

Moreover, as the results show, Ag and Nd codoping hinder the growth of large TiO_2 particles. This causes an increase of the surface area of the catalyst [15]. Furthermore, the suppression in the degree of recombination of electron-hole pairs and decrease in band gap energy of Ag-Nd-TiO_2 (0.75 and 1.5 mol %) samples exhibit more effective electron-hole separation under UV irradiation and improved light absorbing capacity of the catalysts and a higher degree of photocatalytic degradation according to the band gap results. Therefore, the surface redox process by photogenerated electrons and holes takes place more easily and the photocatalytic activity of TiO_2 has significantly improved correspondingly [32].

However, it should also be noted that Ag and Nd particles can act as electron hole recombination centers at higher concentration of dopants, and thus reduce the photocatalytic activity of TiO_2. The probability of electron-hole recombination has been reported to increase by increasing Ag and Nd codoping in TiO_2. Another possible approach is to the excessive Ag and Nd particles, which may occupy the active surface sites of photocatalysts and obstruct the incident light to a certain extent. This results in the inferior efficiencies of these photocatalysts, thereby retarding the charge transfer from the TiO_2 catalyst to MO dye, which is detrimental for the photocatalytic activity [2,42-47].

4. Conclusions

Undoped TiO_2 and Ag-Nd-TiO_2 nanocomposites have been synthesized by sol-gel method using starch as an additive. The synthesized nanocatalysts have been used in photodegradation of methyl orange dye. The red shift, which is observed in band edge absorption peak in UV-Vis absorbance spectrum, occurs by increasing dopant content. Tauc's approach has been used to analyze the band gap of samples and dopant ions and dopant concentrations are very effective on the band gap of TiO_2, as confirmed by calculations. Small amounts of dopants in TiO_2 structure enhance the photodegradation efficiency according to the experimental results obtained in this study. However, further increases of the dopant concentrations lead to decreased photocatalytic activity.

Acknowledgment

We gratefully acknowledge the University of Qom for the support of this work.

References

[1] U. Kurtan, A. Baykal, H. Sozeri, J. Inorg. Organomet. Polym. 25 (2015) 921–929.
[2] A. Bokare, M. Pai, A.A. Athawale, Sol. Energy 91 (2013) 111–119.
[3] J. Wu, Q. Liu, P. Gao, Z. Zhu, Mater. Res. Bull. 46 (2011) 1997-2003.
[4] S. Kohtani, S. Nishioka, E. Yoshioka, H. Miyabe, Catal. Commun. 43 (2014) 61-65.
[5] Y.J. Gu, B. Yan, Inorg. Chim. Acta. 408 (2013) 96-102.
[6] S.A. Sudhir, P.M. Uttamrao, P.A. Dinesh, Nanosci. Nanotechnol. Lett. 5(2013) 968-973.
[7] J. Li, T. Liu, G. Sui, D. Zhen, J. Nanosci. Nanotechnol. 15 (2015) 1408–1415.
[8] M. Harikishoreb, M. Sandhyarani, K. Venkateswarlu, T.A. Nellaippan, N.Rameshbabu, Procedia Mater. Sci. 6 (2014) 557–566.
[9] J.S. Kim, H.J. Sung, B.J. Kim, Appl. Surf. Sci. 334 (2015) 151–156.
[10] S. Rengaraj, S. Venkataraj, J.W. Yeon, Y. Kim, X. Z. Li, G. K. H. Pang, Appl. Catal. B 77 (2007) 157-165.
[11] V. Stengl, S. Bakardjieva, N. Murafa, Mater. Chem. Phys. 114 (2009) 217–226.
[12] B. Khodadadi, M. Bordbar, A. Yeganeh-Faal, J. Sol-Gel Sci. Technol.77 (2016) 521-527.
[13] B. Zhao, Y. W. Chen, J. Phys. Chem. Solids 72 (2011) 1312–1318.
[14] J. Du, H. Chen, H. Yang, R. Sang, Y. Qian, Y. Li, G. Zhu, Y. Mao, W. He, D. J. Kang, Microporous Mesoporous Mater. 182 (2013) 87–94.
[15] J. Du, Z. Wang, G. Zhao, Y. Qian, H. Chen, J. Yang, X. Liu, K. Li, C. He, W. Du, I, Shakir, Microporous Mesoporous Mater. 195 (2014) 167–173.
[16] Y. Kim, M. Yoon, J. Mol. Catal. A: Chem. 168 (2001) 257–263.
[17] C. Lazau, C. Ratiu, C. Orha, R. Pode, F. Manea, Mater. Res. Bull. 46 (2011) 1916–1921.
[18] K.M. Parida, N. Sahu, J. Mol. Catal. A: Chem. 287 (2008) 151-158.
[19] F. Li, Y. Jiang, L. Yu, Z. Yang, T. Hou, S. Sun, Appl. Surf. Sci. 252 (2005) 1410–1416.
[20] M.P. Zheng, M. Gu, Y. Jin, G. Jin, J. Mater. Sci. Eng. B. 77 (2000) 55-59.
[21]. M.P. Zheng, M.Y. Gu, Y.P. Jin, H.H. Wang, P.F. Zu, P. Tao, J.B. He, J. Mater. Sci. Eng. B. 87 (2001) 197-201.
[22] M. Haghighi, K. Nikoofar, Iran. J. Catal. 5 (2015) 57-63.
[23] J. Jiao, Q. Xu, L. Li, J. Colloid Interface Sci. 316 (2007) 596-603.
[24] M. Houmard, D. Riassetto, F. Roussel, A. Bourgeois, G. Berthomé, J.C. Joud, M. Langlet, J. Surf. Sci. 602 (2008) 3364-3374.
[25] B. Khodadadi, M. Sabeti, B. Nahri-Niknafs, S. Moradi-Dehaghi, P. Aberomand-Azar4, S. Raeis-Farshid, Bulg. Chem. Commun. 46 (2014) 624 – 628.
[26] D. Wojcieszak, M. Mazur, M. Kurnatowska, D. Kaczmarek, J. Domaradzki, L. Kepinski, K. Chojnacki, Int. J. Photoenergy (2014) Article ID 463034.
[27] B. Choudhury, B. Borah, A. Choudhury, Mater. Sci. Eng. B 178 (2013) 239– 247.
[28] C. Wang, Y. Ao, P. Wang, J. Hou, J. Qian, Appl. Surf. Sci. 257 (2010) 227–231.
[29] X.C. Liu, E.W. Shi, Z.Z. Chen, H.W. Zhang, B. Xiao, L.X. Song, Appl. Phys. Lett. 88 (2006) 252501–252503.

[30] H. Fu, C. Pan, W. Yao, Y. Zhu, J. Phys. Chem. B 109 (2005) 22432–22439.
[31] R. Liu, P. Wang, X. Wang, H. Yu, J. Yu, J. Phys. Chem. C 116 (2012) 17721−17728.
[32] M. Khodadadi-Moghaddam, Iran. J. Catal. 4 (2014) 77-83.
[33] S. Naraginti, T.V.L. Thejaswini, D. Prabhakaran, A. Sivakumar, V.S.V. Satyanarayana, A.S.A. Prasad, Spectrochim. Acta A 149 (2015) 571–579.
[34] S. Rengaraj, X.Z. Li, J. Mol. Catal. A: Chem. 243 (2006) 60–67.
[35] Y. Yang, J. Wen, J. Wei, R. Xiong, J. Shi, C.X. Pan, ACS Appl. Mater. Interfaces 5 (2013) 6201–6207.
[36] S.W. Chen, J.M. Lee, K.T. Lu, C.W. Pao, J.F. Lee, T.S. Chan, J.M. Chen, Appl. Phys. Lett. 97 (2010) 012104 (1-4).
[37] W. Li, Y. Wang, H. Lin, S.I. Shah, C.P. Huang, D.J. Doren, S.A. Rykov, J.G. Chen, M.A. Barteau, Appl. Phys. Lett. 83 (2003) 4143–4145.
[38] C. Fu, T. Li, J. Qi, J. Pan, S. Chen, C. Cheng, Chem. Phys. Lett. 494 (2010) 117–122.
[39] C. Wang, Y.H. Ao, P. F. Wang, J. Hou, J. Qian, Appl. Surf. Sci. 257 (2010) 227−231.
[40] W. Li, Y. Wang, H. Lin, S. I. Shah, C. P. Huang, D.J. Doren, S.A. Rykov, J.G. Chen, M.A. Barteau, Appl. Phys. Lett. 83 (2003) 4143−4145.
[41] Y.H. Xu, C. Chao, X.L. Yang, X. Li, B.F. Wang, Appl. Surf. Sci. 255 (2009) 8624−8628.
[42] X. Wu, S. Yin, Q. Dong, C. Guo, T. Kimura, J. Matsushita, T. Sato, J. Phys. Chem. C. 117 (2013) 8345−8352.
[43] Z. Wang, C. Chen, F. Wu, B. Zou, M. Zhao, J. Wang, C. Feng, J. Hazard. Mater. 164 (2009) 615–620.
[44] S. Yamamoto, H. Watarai, J. Phys. Chem. C 112 (2008) 12417– 12424.
[45] T.J. Whang, M.T. Hsieh, H.H. Chen, Appl. Surf. Sci. 258 (2012) 2796–2801.
[46] J. Yan, J. Zhang, H. Yang, Y. Tang, Z. Lu, S. Guo, Y. Dai, Y. Han, M. Yao, Sol. Energy 83 (2009)1534-1539.
[47] F. Shirini, S.V. Atghia, M. Alipour Khoshdel, Iran. J. Catal. 1 (2011) 93-97.
[48] B. Khodadadi, M. bordbar, Iran. J. Catal. 6 (2016) 37-42.